Short Communication

Study on MnO₂/MXene-V₂C composite as cathode for magnesium ion battery

Yuan Li[1], Ruinan Zhang[1], Donghui Xu, Dehang Zhang, Yuanchi Wei, Yuxiang Guo[*]

School of Materials and Metallurgy, University of Science and Technology Liaoning, Anshan, 114051, China
[*]E-mail: gyxwsd@126.com

In this paper, the new 2D material MXene-V_2C was prepared by etching V_2AIC. Then, with MXene-V_2C as the base material and $KMnO_4$ as the manganese source, MnO_2/MXene-V_2C composites with different MnO_2 content are prepared by one-step hydro-thermal method. After a series of characterization analysis of the prepared samples, the results show that MnO_2/MXene-V_2C has the best performance when MnO_2 content is 20%. As shown from the results, when the charging and discharging current is 100mA/g, the first discharge capacity of the composite is up to 130mAh/g, which is 2.4 times as much as that of MnO_2 as the cathode material alone, and it decays to 41% after 100 cycles, which is close to the first discharge specific capacity of MnO_2. The adding of the MXene-V_2C increases the conductivity and stability of MnO_2.

1. INTRODUCTION

The rapid development of society causing to the increasing demand for energy day by day. The use of conventional energy (oil, coal, natural gas and other fossil fuels) will seriously pollute environment and the earth's reserves are limited. The utilization of renewable energy, such as solar energy, wind energy and geothermal energy, provides research direction for the problem of energy shortage[1-2]. However, these energies are intermittent and more effectively applied by converting into electric energy, and it is especially important for the electric energy storage device to converse the intermittent energy[3-4]. Therefore, the new high-capacity environmental protection secondary battery is favored by the majority of researchers at home and abroad, so efficient energy conversion and storage of the secondary battery has become an important research topic in the field of battery energy in the world[5-6]. At present, the secondary batteries are mainly adopted nickel cadmium, lead-acid and

lithium-ion batteries, but the first two batteries contain harmful elements, which will pollute the environment and have a low safety factor[7-8]. Lithium-ion battery is the most widely used battery energy in our life due to the advantages of high energy density, and high technology maturity, but exists the high preparation cost and poor safety and other shortcomings[9-11]. Therefore, it is particularly important for the research and development of clean and safe new energy. According to the diagonal principle, some researchers found that magnesium and lithium, as diagonal elements on the periodic table of elements, is similar in physical and chemical properties, and for unique resources development advantages of the large reserves and security, magnesium ion battery is very likely to become a new type of green energy battery in the future[12].

Magnesium ion battery is mainly composed of three parts, including a positive active material in which magnesium ions can be embedded and released, an electrolyte used to conduct magnesium ions, and a negative electrode of the metal magnesium or magnesium alloy[13-14]. Due to the similar working principle with lithium ion battery, when the battery is discharged, the magnesium ion battery's metal magnesium on the negative electrode surface converts into magnesium ion and enters the electrolyte, moves to the positive electrode surface and embeds into the positive material; when the battery is charged, the magnesium ion embedded into the positive material is released to Mg anode and then electrode is deposited on the negative surface of the magnesium[15-16]. Although the working principle of magnesium ion battery is very similar to that of lithium ion battery, there are still great differences between them[17-19]. During the charging and discharging process of lithium-ion battery, there will be a dense passivation film on the surface of electrode material, but lithium ion can still cross freely[20]. Magnesium ion battery will also produce passivation film in operation, but the magnesium ion of non-conductive will greatly reduce the cycling performance of magnesium ion battery. But the high charge energy of magnesium ions in magnesium ion battery produces strong polarization in the process of transmission, as a result, when the magnesium ions embedded into a lot of material, it will be subject to strong resistance, and difficult to carry out reversible insertion and ejection, so the choice of magnesium ion battery anode materials is strictly limited, thus the most important issue finds good reversible embedding and emergence of active material, directly affecting the cycle performance of magnesium ion battery and charge and discharge capacity[21-23].

Currently, the research on the cathode materials of magnesium ion battery is still in the initial stage at home and abroad, and still has some problems such as poor conductivity, poor cycle performance and so on[24]. According to the existing report about materials for magnesium ion batteries, the transition metal oxides are the most commonly, among of which Manganese dioxide is the most studied[25-26]. MnO_2, as a kind of electrode material with high theoretical specific capacity, low cost and easy obtaining, has been widely used as the electrode material of battery[27-29]. However, when MnO_2 is used as the anode material of magnesium ion battery alone, it has the disadvantages of poor conductivity and poor cycle performance. In view of these problems, some researchers will composite it with some materials with good conductivity to improve its performance study[30-33].

MXene is a novel graphene type' 2D transition metal carbide and carbonitride, which its general formula is $M_{n+1}X_nT_x$ (n = 1, 2, 3, M is transition metal element, X is carbon or nitrogen element, TX is surface groups such as O^{2-}, OH^-, F^-, NH_3, and NH^{4+})[34-35]. This material has large specific surface area, high conductivity and stable chemical properties. In addition, the hydrophilic surface of MXene material

is able to be well moistening electrolyte solution[36]. The similar 2D stratified structure between the MXene and graphene provides a good transport path for the movement of ions. Meanwhile, this material owns the good conductivity, flexibility and large specific surface area, leading to a new research direction for its application in portable electronic equipment and structural energy storage equipment[37-39]. It is a very valuable and potential electrode material[40]. So far, in MXene series materials, MXene-V_2C is electrode material that is most widely studied and widely used, and successfully used as electrode materials for super-capacitors, lithium-ion batteries and sodium ion batteries, and has excellent capacity and rate performance[41]. But the research of magnesium battery has not been reported. In this paper, based on this advantage of MXene, we use MXene-V_2C as a substrate material, composite with different proportions of MnO_2, and its composite material as cathode material for magnesium ion battery for electrochemical performance study.

2. EXPERIMENT

2.1 Preparation of MXene-V_2C materials

The forebody MAX phase material V_2AlC is milled in an agate mortar to reduce particle size. The ground V_2AlC material is placed in a beaker and dried at 75℃ for 2h in a blast drying oven. Add 2g of NaF, 40ml of HCl and 40mL of distilled water into the beaker, and stir at room temperature for 15min to make the medicine dissolve and mix evenly. Take 1.44g of the dried V_2AlC material and pour it into the mixed solution. Heat it in a constant temperature magnetic stirrer to 90℃ for etching reaction for 72h. Carry out centrifugal washing repeatedly the etched solution in a high-speed centrifuge until the pH of the solution after centrifugal was close to neutral. Pour out the supernatant fluid, dry the precipitate in the vacuum drying oven at 80℃ for 24 hours, and finally dry the solid sample in the drying oven, which is MXene-V_2C materials.

2.2 Preparation of MnO_2/MXene-V_2Ccomposite materials

Accurately weigh 0.2g of MXene-V_2C material, pour it into a beaker with 30ml distilled water to ultrasonically disperse for 45min until the solution without obvious particle solid agglomeration. Weigh a certain amount of $KMnO_4$ into the beaker, add 40mL distilled water and stir on the magnetic until it is completely dissolved. Then pour the dissolved $KMnO_4$ solution into the evenly dispersed MXene-V_2C dispersion and stir on the magnetic agitator for 50min until the mixture is evenly mixed. Finally, pour the mixed solution into a 100ml hydrothermal reactor for reaction and in the air blast drying oven at 150 ℃ for 8h, cool it to room temperature after the reaction. At last centrifugal wash the solution after the reaction to pH 6-7, place the precipitate in the drying oven and dry it at 100 ℃ for 6h. The composite of MnO_2/MXene-V_2C is obtained. In the MnO_2/MXene-V_2C composite materials prepared in this paper, the MnO_2 contents in the respective composite materials are 20%, 50% and 80% respectively. In the preparation of different composite materials, the mass of MXene-V_2C is fixed, but only the amount of $KMnO_4$ added is changed.

2.3 Material Characterization

X' Pert Powder X-ray diffractometer (Cu Target Kal radiation, current: 40 mA, voltage: 40 kV, scanning speed: 4° /min, scanning angle: $2\theta=10°\sim90°$) was used to deal with the phase analysis towards the sample. Microstructure and morphology of the prepared samples were observed by HD field emission scanning electron microscopy (SEM).

2.4. Test of Electrochemical Performance

Active materials, conductive black and PVDF were dispersed in the N-methyl-2-pyrrolidone (NMP) at a mass ratio of 8:1:1. The slurry after fully grinding was evenly coated on the copper foil. The electrode material was dried at 110℃ in the vacuum oven for 12h and then put it on the powder compressing machine for tablet compressing. The quality before and after coating the copper foil was weighed and the mass of active material was calculated. After all these steps, the electrode material was put into the glove box for use. In the glove box, the CR2032 button battery was assembled from bottom to top according to the sequence of negative shell, magnesium sheet, electrolyte (APC), fiberglass diaphragm, electrolyte, positive electrode, gasket, spring sheet and positive shell. Then pressed and sealed it. The sealed battery would be tested for its electrochemical performance after standing for 6 hours. The charge-discharge test was carried out on the LAND battery test system. The test temperature was 25℃ and the cut-off voltage was 0.01~2.0V (vs. Mg/Mg^{2+}).

3. RESULTS AND DISCUSSION

3.1 XRD and SEM Analysis

Figure.1 shows the XRD patterns of MXene-V_2C, MnO_2 and MnO_2/MXene-V_2C composites with different MnO_2 mass ratio. It can be seen that MXene-V_2C has obvious diffraction peaks at $2\theta =$ 13.56°, 41.30°, 55.57°, 75.17° and 78.87°, which is the characteristic diffraction peak of MXene-V_2C, and consistent with other literature reports[42-43]. At $2\theta=12.3$°, 24.8° and 36.6°, MnO_2 has obvious characteristic diffraction peak without impurity peak, which corresponds to the PDF card JCPDS 01-086-0666[44-46]. The sample belongs to rhombic crystal system, with R-3m(166) spatial point group structure and stratified structure MnO_2, belonging to hydrated MnO_2 with potassium[47-49]. The XRD patterns of MnO_2/MXene-V_2C composite keep the diffraction peaks of MXene-V_2C and MnO_2. It can be seen that MXene-V_2C and MnO_2 in the composite keep their own crystal structure without any change. With the increase of MnO_2 content in composites, some characteristic diffraction peaks of MXene-V_2C gradually weaken, while characteristic peaks of MnO_2 gradually appear. The MnO_2 content is 80% in the composite material, the diffraction peaks of MXene-V_2C are the weakest, some characteristic diffraction peaks disappear, and the diffraction peaks of MnO_2 are the strongest, accounting for the main components. In conclusions, hydro-thermal method achieves to prepare the MnO_2 and MXene-V_2C composite materials, and with the increase of MnO_2 content in composites, MnO_2 covers up the MXene-V_2C new layered materials. When the MnO_2 content is 20% in the

composite material, the diffraction peaks of MnO_2 nanoparticles and MXene-V_2C layered materials are the strongest with the best composite effect.
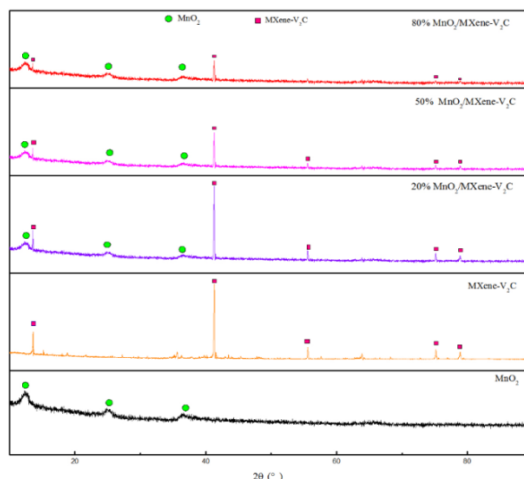
Figure 1. XRD Spectrum of MnO_2, MXene-V_2C and MnO_2/MXene-V_2C with different MnO_2 contents

Figure.2 shows SEM pictures of MXene-V_2C, MnO_2 and MnO_2/MXene-V_2C composites with different MnO_2 contents. Figure (a) shows that MXene-V_2C has a typical layered structure, the layers with smooth surface are separated from each other, so the large specific surface area of MXene-V_2C can not be fully utilized[50-52]. Figure (b) shows the SEM image of MnO_2, MnO_2 is a 3D bract shaped flower ball with a diameter of 180-190nm, formed by overlapping and agglomeration of layers. The rich void structure of these flower balls is conducive to the insertion and removal of ions[53-55]. Figure (c-e) shows the SEM picture of MnO_2/MXene-V_2C composites with different MnO_2 contents, Figure (c) is the SEM picture of MnO_2/Mxene-V_2C composite with 20% MnO_2 content. We can see that MnO_2 adheres to the surface and inter-layer of MXene-V_2C, increasing the inter-layer spacing of MXene-V_2C, which is conducive to the in and out of ions. Figure (d-e) is the SEM picture of MnO_2/MXene-V_2C composite with 50% and 80% MnO_2 contents. In the pictures, MnO_2 particles are tightly covered on the surface of MXene-V_2C and filled in the inter-layer gap of MXene-V_2C, which seriously hinders the in and out of inter-layer ions.
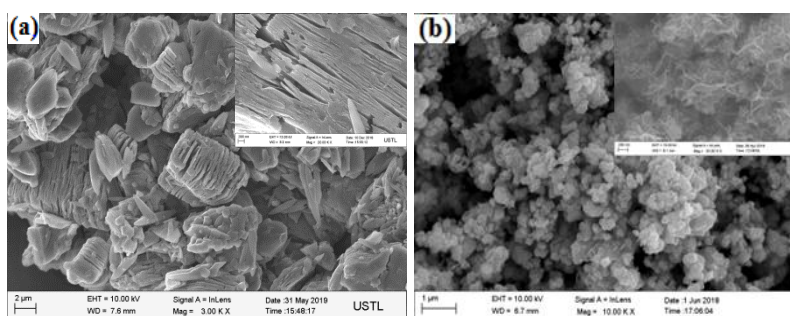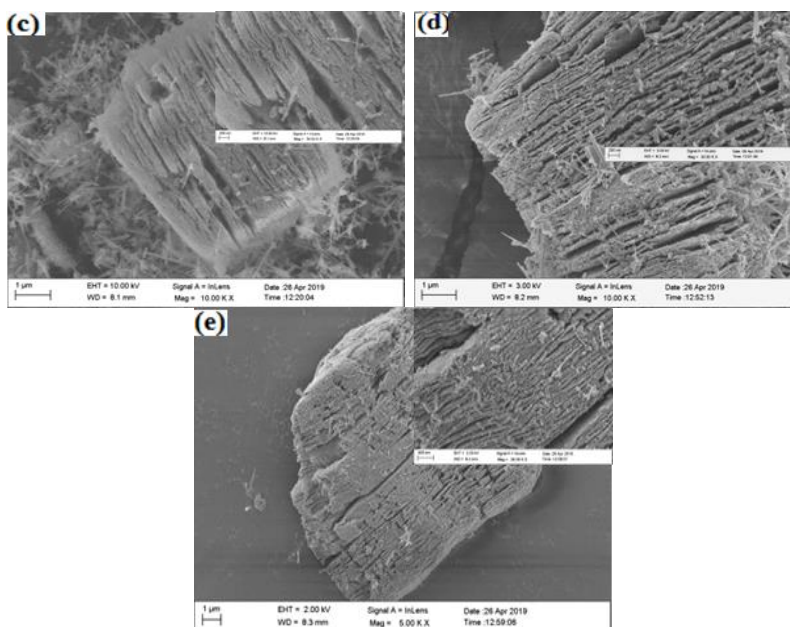
Figure 2. (a) SEM picture of MXene-V_2C material; (b) SEM picture of MnO_2 material; (c)-(e) SEM pictures of MnO_2/MXene-V_2C composites with 20%、50% and 80% MnO_2 contents

In conclusion, in MnO_2/MXene-V_2C composites with different MnO_2 contents, with the increasing mass proportion of MnO_2, the surface and inter-layer of MXene-V_2C laminated materials will be more and more seriously filled and wrapped by MnO_2. MnO_2 content accounted for 80% of the composite material, the interval between layers of MXene-V_2C materials will be blocked, ions cannot be smoothly embedded and removed, and the characteristics of layered structure of MXene-V_2C materials will not fully play, affecting the electrochemical performance. At the MnO_2/MXene-V_2C composite with 20% MnO_2 content, MnO_2 and MXene-V_2C realize complementary advantages, and the both of them are combined evenly, which is conducive to the in and out of ions.

3.2 Analysis of Electrochemical Performance
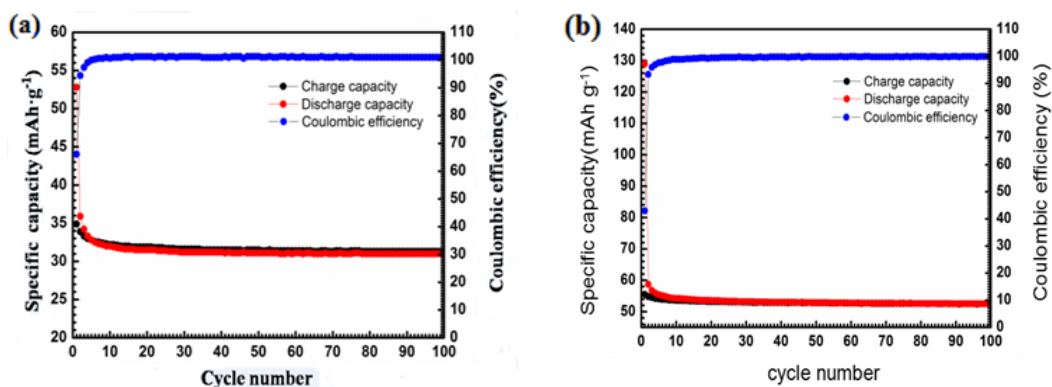
Figure 3. Cycle performance of (a)MnO_2 and (b)MnO_2/MXene-V_2C composites with 20% MnO_2 content

Figure.3 shows the constant current charge and discharge test of MXene-V_2C, MnO_2 and MnO_2/MXene-V_2C composites with different MnO_2 contents. Figure.3 (a) shows at the current density

of 50mA/g, the first discharge capacity of MnO_2 is only 53mAh/g, and the discharge capacity after 100 cycles is 32mAh/g. With the increase of the number of cycles, the specific discharge capacity decreases gradually. In the whole charging and discharging, the coulomb efficiency is close to 100%. Figure.3 (b) shows when the MnO_2/MXene-V_2C composites with 20% MnO_2 content are used as positive materials for magnesium batteries, the first discharge capacity is up to 130 mAh/g, 2.4 times as much as that of pure MnO_2, and is reduced to 59mAh/g after 100 cycles. Meanwhile, the specific discharge capacity is also higher than that of pure MnO_2, and the cycle performance is better than that of MnO_2. The appropriate MnO_2 in MnO_2/MXene-V_2C composites both plays a role in expanding layers of MXene-V_2C during the reaction process, and fully play the high conductivity of MXene-V_2C materials.

Figure.4 shows the voltage and capacity curve of MnO_2 and MnO_2/MXene-V_2C composite with MnO_2 content of 20%. The test voltage range is 0.2V-2.0V, and the current density is 50mA/g. Figure.4 (a) shows the first discharge capacity and charging capacity of MnO_2 are 53mAh/g and 37mAh/g respectively, and the capacity shows a large amount of attenuation after the second cycle. The first discharge capacity and charge capacity of MnO_2/MXene-V_2C composite are 130 mAh/g and 63mAh/g respectively. Both of their first discharge capacity is larger than the charge capacity, and there is no voltage platform in the first charge and discharge. With the increase of cycle times, it tends to be gentle. When MnO_2/MXene-V_2C composite is used as the positive electrode of Mg ion battery, the charge-discharge capacity is higher and the time is longer. It shows that the magnesium ion can be embedded and separated more deeply by adding MXene-V_2C material.
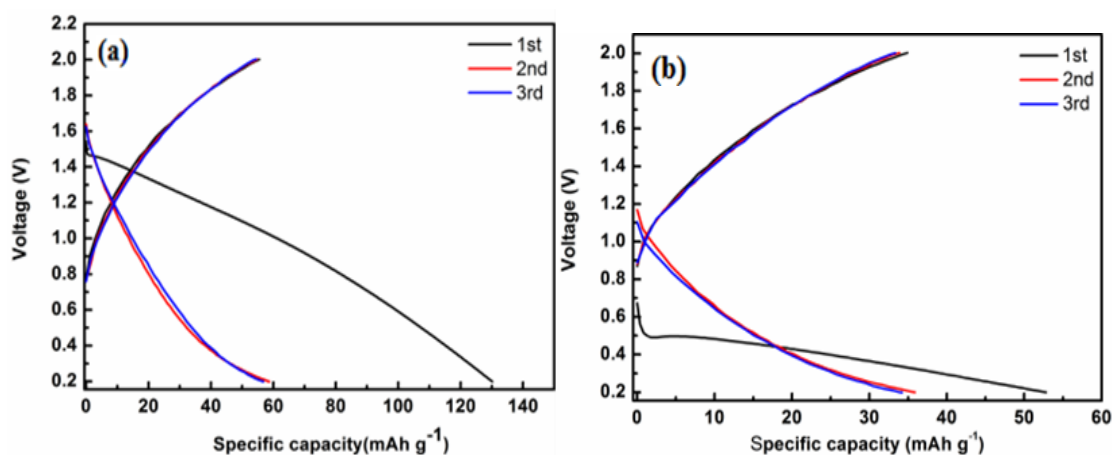
**Figure 4.** Charge and discharge curves of (a)MnO_2 and (b)MnO_2/MXene-V_2C materials with 20% MnO_2 content

Fig.5 shows the CV curve of MnO_2/MXene-V_2C composite material with MnO_2 content of 20% in the voltage range of -1.2V-0.6V. Compared with MnO_2, MnO_2/MXene-V_2C composite responses more obvious anode and cathode current with larger CV area and obvious capacity. This is consistent with the relatively flat discharge curve shown in the low voltage area in Figure 4. In figure, after the smooth reaction, CV curve shows with the increase of the number of cycles, the capacity gradually increased and finally reached a stable and moderate state. At this point, the main capacity is mainly contributed by

the addition of MnO_2/MXene-V_2C material in MnO_2/MXene-V_2C composite material, and the volume of MnO_2/MXene-V_2C will expand to a certain extent after MnO_2 reaches a stable state, at which point the expandable of the layer gap of MnO_2/MXene-V_2C layered material will is more conducive to the in and out of magnesium ions and improves the capacity contribution of MXene-V_2C material.
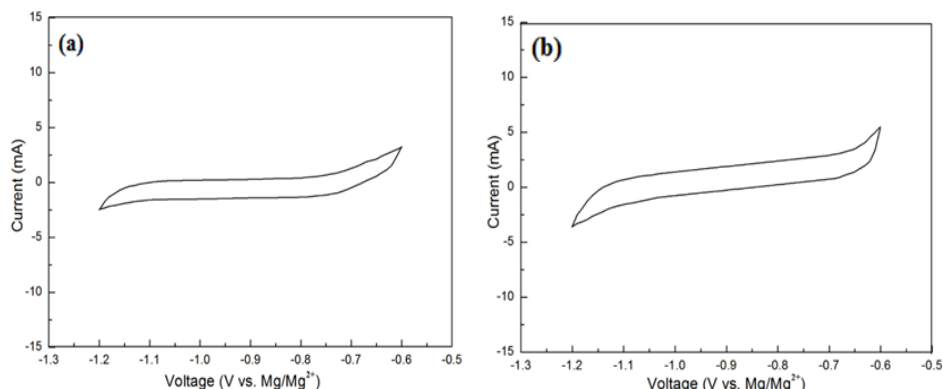
Figure 5. (a) CV diagram of MnO_2 and (b)MnO_2/MXene-V_2C composite material with 20% MnO_2 content

The rate performance of MnO_2 and MnO_2/MXene-V_2C composite with MnO_2 content of 20% were shown in Figure.6. Under the high current density of 100mA/g, 200mA/g and 500mA/g, the capacity of MnO_2/MXene-V_2C composite is 65mAh/g, 40mAh/g and 25mAh/g respectively, which is much higher than that of MnO_2 under different current density. The figure shows that when the number of cycles is less than 10, the degree of capacity reduces relatively obviously. In the process of initial discharge, the electrostatic effect of magnesium ion on electrostatic effect with electrode material causes that the magnesium ion is easy to attach to the active position of electrode material. At a high current density of 500 mA/g, the battery still has a stable capacity of 25 mAh/g and a high capacity in a wide range of current density, which indicates that MnO_2/MXene-V_2C is a very good cathode material for magnesium battery.
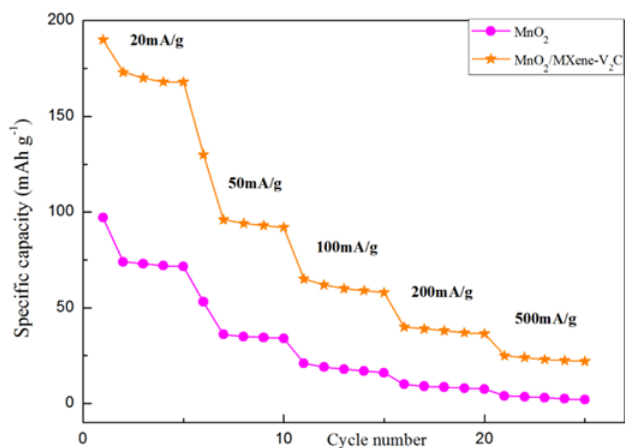
Figure 6. Rate performance of MnO_2 and MnO_2/MXene-V_2C composites with 20% MnO_2 content

Table 1. Comparison with other cathode materials for magnesium battery.

Cathode material	Electrolyte	Capacity (mAh/g)	References
MnO_2(Hollandite)	$Mg(ClO_4)_2$/AC	85	[56-57]
MnO_2 (Birnessite)	$Mg(ClO_4)_2$	65	[58-59]
MnO_2 (Spinel)	$Mg(ClO_4)_2$	80	[60]
MnO_2 (Spinel)	APC	64	[61]
MnO_2/MXene-Ti_3C_2	APC	105	[61]
TiS_2	APC	58	[62-65]
TiS_2/MXene-Ti_3C_2	APC	97	[65]
V_2O_5	$Mg(ClO_4)_2$/THF	50	[66-69]
MoS_2	$Mg(AlClBu)_2$/THF	22	[70-71]
MnO_2/MXene-V_2C	APC	130	In this ppaper

Table 1 compares the electrochemical performance of some transition metal oxide sulfides and the composite materials combined with MXene as the positive electrode of magnesium ion batteries. Compared with the cathode material shown in Table 1 above, when the electrolyte is $Mg(ClO_4)_2$ solution, the charge-discharge maximum capacity of pure MnO_2 is 85mAh/g. In the APC electrolyte it's only 64mAh/g. After adding MXene-Ti_3C_2 material, the charge and discharge capacity is 105mAh/g. Similarly, the capacity of TiS_2/Mxene-Ti_3C_2 composite material added with MXene has also been greatly improved. In this paper, MnO_2/MXene-V_2C composite materials were prepared with a charge and discharge capacity up to 130mAh/g. Its electrochemical performance is even better than MXene-Ti_3C_2. This is because MXene-V_2C nanosheet with better conductivity provides a looser structure for the entry and exit of magnesium ions, thus providing more active sites for the storage of magnesium ions, and shortening the diffusion path of magnesium ions.

4. CONCLUSION

In this paper, the MnO_2/MXene-V_2C composites with different MnO_2 contents were successfully prepared. And when the content of MnO_2 is 20%, the compound effect is the best. MnO_2/MXene-V_2C composites with 20% MnO_2 content are used as the cathode material of magnesium ion battery, and its electrochemical performance are tested. The results show that when the charge-discharge current is 100mA/g and voltage range is 0.22V, the first discharge capacity of the composite is 2.4 times as much as that of MnO_2 as the positive material alone, and up to 130mAh/g. After 100 cycles, it decays to 41% of the original value with equal to the first discharge specific capacity of MnO_2. And MXene-V_2C base material has better electrochemical performance than MXene-Ti_3C_2 material. For the research of new electrode materials, MXene series materials have great research significance.

CONFLICTS INTEREST
There are no conflicts to declare.

References

1. Z. Yang, J. Zhang and M. Kintner, *Chem. Rev.,* 111 (2011) 3577.
2. Y. Li, D.H. Xu, D.H. Zhang,D.L. Qu and Y.X. Guo, *Int. J. Electrochem. Sci.*,14 (2019) 11102.
3. B. Dunn, H. Kamath and J.M. Tarascon*, Science*, 334 (2011) 928.
4. J. Cui, T.G. Zhan, and K.D. Zhang, *Chin. Chem. Lett*., 28 (2017) 2171.
5. Y. Li, D.H. Xu, D.H. Zhang and Y.X. Guo, *RSC Adv*., 9 (2019) 33572.
6. D. Aurbach, Z. Lu, Y Gofer and A. Schechter, *Nature*, 407 (2000) 724.
7. J.O. Besenhard and M. Winter*, ChemPhys Chem,* 3 (2002) 155.
8. O.R. Brown and R. McIntyre, *Electrochim. Acta*, 30 (1985) 627.
9. T.D. Gregory, R.J. Hoffman and R.C. Winterton, *J. Electrochem. Soc*., 137 (1990) 775.
10. Huie, D.C. Bock and E.S. Takeuchi, *Coord. Chem. Rev*., 287 (2015) 15.
11. H.D. Yoo, Y. Liang, H. Dong, J.H. Lin, H. Wang and Y.S. Liu, *Nat. Commun*., 8 (2017) 339.
12. N. Amir, Y. Vestfrid, O. Chusid and Y. Gofer, *J. Power Sources*, 174 (2007) 1234.
13. D. Aurbach, G.S. Suresh, E. Levi, A. Mitelman, O. Mizrahi, O. Chusid and M. Brunelli, *Adv. Mater.*, 19 (2007) 4260.
14. O. Chusid, Y. Gofer, H. Gizbar, Y. Vestfrid, E. Levi and D. Aurbach, *Adv. Mater*., 15 (2003) 627.
15. M. Inamoto, H. Kurihara and T Yajima, *Electrochemistry,* 80 (2012) 421.
16. D. Aurbach, Y. Gofer, Z. Lu, A. Schechterc, O. Chusida, H. Gizbara, Y. Cohena, V. Ashkenazia, M. Moshkovicha and and E. Levi, *J. Power Sources*, 97 (2001) 28.
17. M. Levi, E. Lancry, E. Levi, H. Gizbar, H. Gofer and D. Aurbach, *Solid State Ionics*, 176 (2005) 1695.
18. E. Levi, Y.Gofer, Y. Vestfreed, E. Lancry and D. Aurbach, *Chem.Mater*., 14 (2002) 2767.
19. A. Mitelman, M. Levi, E. Lancry, E. Levi and D. Aurbach, *Chem.Commun*., 41 (2007) 4212.
20. M.H. Matthew, C.B. David, S.T. Esther, C.M. Amy and J.T. Kenneth, *Coord. Chem. Rev*., 287 (2015) 15.
21. D. Aurbach, I Weissman and Y Gofer, *The Chem Record*, 3 (2003) 61.
22. Y.N. Nuli, J. Yang, Y.S. Li and J.L. Wang, *Chem. Commu*n., 46 (2010) 3794.
23. H.S. Kim, T.S. Arthur, G.D. Allred, J. Zajicek, J.G. Newman, A. E. Alexande and A.G. Oliver, *Nat. Commun.,* 2 (2011) 427.
24. E. Strauss, D. Golodnitsky and E. Peled, *Electrochim. Acta*, 45 (2000) 1519.
25. B. Prélot, F. Villiéras, M. Pelletier, F. Thomas and C. Poinsignon, *J. Colloid Interface Sci*., 264 (2003) 343.
26. M.M. Thackeray, *Prog. Solid State Chem*., 25 (1997) 1.
27. O. Ghodbane, J.L. Pascal, F. Favier, *ACS Appl. Mater. Interfaces*, 1 (2009) 1130.
28. L. Athouel, F. Moser, R. Dugas, O. Crosnier, D. Belanger and T. Brousse. *J. Phys. Chem*. C, 112 (2008) 7270.
29. R. Zhang, X. Yu and K.W. Nam, *Electrochem. Commun*., 23 (2012) 110.
30. A. Yamada, M. Tanaka, K. Tanaka, S. Koji, *J. Power Sources*, 81 (1991) 73.

31. T.S. Arthur, R. Zhang, C. Ling and P.A. Glans, *ACS Appl. Mater. Interfaces*, 6(2014) 7004.
32. J.S. Kim, W.S. Chang, R.H. Kim, D.Y. Kim, D.W. Han, K.H. Lee and S.G. Doo, *J. Power Sources*, 273 (2015) 210.
33. A. Bahloul, B. Nessark, F. Habelhames and C.M. Julien, *Ionics,* 17 (2011) 239.
34. M.W. Barsoum, *Prog. Solid State Chem.*, 28 (2000) 201.
35. M. Ghidiu, M.R. Lukatskaya and M.Q. Zhao, *Nature*, 516 (2014) 78.
36. M. Naguib, M. Kurtoglu, V. Presser, J. Lu, J.J. Niu, M. Heon, L. Hultman and Y. Gogotsi, *Adv. Mater.,* 23 (2011) 4248.
37. D. Sun, Q. Hu, and J. Chen, *ACS Appl. Mater. Interfaces*, 8 (2016) 74.
38. Y. Dall'agnese, P.L. Taberna, Y. Gogotsi and P. Simon, *J. Phys. Chem. Lett.*, 6 (2015) 2305.
39. E.H. Kisi, E. Wu, J.S. Zobec, S. Jennifer and P. Riley, *J. Am. Ceram. Soc.*, 90 (2010) 1912.
40. X. Zhang, X.D. Zhao, D.H. Wu, Y. Jing and Z. Zhou, *Nanoscale,* 7 (2015) 16020.
41. M. Naguib, J. Come, B. Dyatkin, D. Boris and P. Volker, *Electrochem. Commun.*, 16 (2012) 61.
42. M. Khazaei, M. Araim and T. Sasaki, Adv. Funct. Mater., 23(2012) 2815.
43. Y. Xie, M. Naguib and V. N. Mochalin, *J. Am. Chem. Soc.*, 136(2014) 6385.
44. L. Lu, X. Han, J. Li, J. Hua and M.O Yang, *J Power Sources*, 226 (2013) 272.
45. J. Xie, X.Wang and A. LI, *Corros. Sci.*, 60 (2012) 129.
46. M. Nguib, V. Presser and N. Lane, *RSC Adv.*, 1 (2011) 1493.
47. S. Devaraj and N. Munichandraiah, *J. Phys. Chem. C*, 112 (2008) 4406.
48. T. Brousse, M. Toupin and R. Dugas, *J. Electroanal. Chem.*, 153 (2006) A2171.
49. S. L. Kuo and N. L. Wu, *J. Electroanal. Chem.*, 153 (2006) A1317.
50. X. Wang, S. Kajiyama, H. Iinuma and A. Yamada, *Nat. Commun.*, 6 (2015) 1.
51. F. Shahzad, M. Alhabeb, C. B. Hatter, S. M. Hong, C. M. Koo and Y. Gogotsi, *Science*, 353 (2016) 1137.
52. Y. Qing, W. Zhou, F. Luo and D. Zhu, *Ceram. Int.*, 42 (2016) 16412.
53. C. J. Xu, H. D. Du and B. H. Li, *J. Electrochem. Soc.*, 156 (2009) A73.
54. O. Ghodbane, J. L. Pascal and F. Favier, *ACS Appl. Mater. Interfaces*, 1 (2009) 1130.
55. C. E. Ren, K. B. Hatzell, and Y. Gogotsi, *J. Phys. Chem. Lett.*, 6 (2015) 4026.
56. M. Naguib, J. Come, B. Dyatkin, V. Presser, P.L. Taberna, P. Simon, M.W. Barsoum and Y. Gogotsi, *Electrochem. Commun.*, 16 (2012) 61.
57. Z. Lin, D. Sun, Q. Huan, J. Yang, M.W. Barsoum and X. Yan, *J. Mater. Chem. A*, 3 (2015) 14096.
58. F. Shahzad, M. Alhabeb, C.B. Hatter, B. Anasori, S.M. Hong, C.M. Koo and Y. Gogotsi, *Science*, 353 (2016) 1137.
59. Y. Qing, W. Zhou, F. Luo and D. Zhu, *Ceram. Int.*, 42 (2016) 16412.
60. J. Chen, Z.L. Tao and S.L. Li, *Angew. Chem., Int. Ed.*, 42 (2003) 2147.
61. Y. Li, Y.X. Guo, D. H. Xu and D.H. Zhang, *RSC Advances.,* 9 (2019) 33572.
62. P.G. Bruce, F. Erok, and J. Nowinski, J. Mater. Chem., 1 (1991) 705.
63. P.G. Bruce, F. Erok, and P. Lightfoot, Solid State Ionics, 53 (1992) 351.
64. P. Lightfoot, F. Erok, and J.L. Nowinski, J. Mater. Chem. A, 2 (1992) 139.
65. Y. Li, Y.X. Guo, D. H. Xu and D.H. Zhang, *Int. J. Electrochem. Sci.,* 14 (2019) 11102.
66. L. Yu and X. Zhang, J. *Colloid Interface Sci.*, 278 (2004) 160.
67. P.E. Tang, J.S. Sakamoto, E. Baudrin and B. Dunn, *J. Non-Cryst. Solids*, 350 (2004).
68. I. Stojkovic, N. Cvjeticanin, S. Markovic and S. Mentus, *Acta Phys. Pol. A*, 117 (2010) 837.
69. J.P. Pereira-Ramos, R. Messina and J. Perichon, *J. Electroanal. Chem.*, 218 (1987) 241.
70. Y. Liu, L. Jiao, Q. Wu, Y. Zhao, K. Cao, H. Liu, Y. Wang, and H. Yuan, Nanoscale, 5 (2013) 9562.
71. 35. S. Yang, D. Li, T. Zhang, and Z. Tao, *J. Phys. Chem. C*, 116 (2012) 1307.